Tamm's problem in the Schwinger and exact approaches

2000 J. Phys. A: Math. Gen. 33 7585

(http://iopscience.iop.org/0305-4470/33/42/308)

J. Phys. A: Math. Gen. **33** (2000) 7585–7606. Printed in the UK PII: S0305-4470(00)12197-3

Tamm's problem in the Schwinger and exact approaches

G N Afanasiev†§, V G Kartavenko† and J Ruzicka‡

† Bogoliubov Laboratory of Theoretical Physics, Joint Institute for Nuclear Research, Dubna, Moscow District, 141980, Russian Federation
‡ Faculty of Mathematics and Physics, Comenius University, 84215, Bratislava, Slovakia

E-mail: afanasev@thsun1.jinr.ru

Received 1 March 2000

Abstract. Schwinger's approach gives a fresh look on Tamm's problem (charge, being initially at rest, exhibits an instant acceleration, moves with a finite velocity, and, after an instant deceleration, goes to the state of rest). Schwinger's angular and frequency distributions are compared with Tamm's ones which in turn are compared with exact distributions. Criteria for the validity of Tamm's formulae are checked by numerical calculations.

1. Introduction

The aim of this consideration is to analyse frequency and angular distributions of a radiation in the so-called Tamm problem. The latter treats the point charge as at rest in a medium at the space point $z = -z_0$ up to a moment $t = -t_0$. In the time interval $-t_0 < t < t_0$ the charge moves with velocity v that can be smaller or greater than the velocity of light in the medium, c_n. After the moment $t = t_0$ the charge is again at rest at the point $z = z_0$. This problem was first considered by Tamm [1] in 1939. Later, it was analysed by qualitatively Lawson [2, 3] and numerically by Zrelov and Ruzicka [4, 5]. In 1996, the exact solution of Tamm's problem was found for the non-dispersive medium [6]. A careful analysis of this solution was given in [7]. It was shown there that Tamm's formulae do not describe Cherenkov radiation (CR) properly. On the other hand, Schwinger [8] suggested evaluating frequency and angular spectra of the radiation produced by an arbitrarily moving charge without explicitly using the electromagnetic field strengths. This method was successfully applied to the consideration of synchrotron motion [9, 10].

In this consideration, we compare Tamm's and Schwinger's approaches between themselves and with an exact solution of Tamm's problem.

The plan of our exposition is as follows. In section 2, we reproduce Tamm's frequency and angular distributions of the radiation produced by a point charge moving uniformly on a finite space interval. In section 3, by applying Schwinger's method to the consideration of Tamm's problem we obtain the instant (i.e. at a given moment of time) angular and frequency distributions of the radiated power. The integration of the angular distribution over time motion gives the angular-frequency distribution of the energy radiated for a finite time interval. Performing angular integration, one obtains the frequency distribution of the energy radiated for a finite time interval. In particular cases one arrives either at Tamm–Frank or Tamm

§ Author to whom correspondence should be addressed.

0305-4470/00/427585+22$30.00

formulae. The exact electromagnetic fields of Tamm's problem are given in section 4. They are compared with the famous Tamm formula describing the angular-frequency distribution of the radiated energy. Criteria for the validity of Tamm's formula are given. These criteria are checked by the numerical calculations presented in the same section.

2. Tamm's original approach

Tamm considered the following problem. A point charge is at rest at the point $z = -z_0$ of the z-axis up to a moment $t = -t_0$. In the time interval $-t_0 < t < t_0$ it moves uniformly along the z-axis with velocity v greater than the velocity of light in the medium c_n. For $t > t_0$, the charge is again at rest at the point $z = z_0$. The non-vanishing Fourier component z of the vector potential (VP) is given by

$$A_\omega = \frac{1}{c}\int_{-z_0}^{z_0} \frac{1}{R} j_\omega(x', y', z') \exp(-\mathrm{i}\omega R/c_n)\,\mathrm{d}x'\,\mathrm{d}y'\,\mathrm{d}z'$$

where $R = [(x-x')^2 + (y-y')^2 + (z-z')^2]^{1/2}$, $j_\omega = 0$ for $z' < -z_0$ and $z' > z_0$ and $j_\omega = e\delta(x')\delta(y')\exp(-\mathrm{i}\omega z'/v)/2\pi$ for $-z_0 < z' < z_0$. Inserting all of this into A_ω and integrating over x' and y', one finds

$$\begin{aligned} &A_\omega(x, y, z) = \frac{e}{2\pi c}\int_{-z_0}^{z_0} \frac{\mathrm{d}z'}{R} \exp\left[-\mathrm{i}\omega\left(\frac{z'}{v} + \frac{R}{c_n}\right)\right] \\ &R = [\rho^2 + (z-z')^2]^{1/2} \qquad \rho^2 = x^2 + y^2. \end{aligned} \tag{2.1}$$

At large distances from the charge ($R \gg z_0$) one has $R = R_0 - z'\cos\theta$, $\cos\theta = z/R_0$, $R_0 = (x^2 + y^2 + z^2)^{1/2}$. Inserting this into (2.1) and integrating over z' one obtains

$$\begin{aligned} &A_\omega(\rho, z) = \frac{e\beta q(\omega)}{\pi R_0 \omega}\exp(-\mathrm{i}\omega R_0/c_n) \qquad q(\omega) = \frac{\sin[\omega t_0(1-\beta_n\cos\theta)]}{1-\beta_n\cos\theta} \\ &\beta = \frac{v}{c} \qquad \beta_n = \frac{v}{c_n} \qquad t_0 = \frac{z_0}{v}. \end{aligned} \tag{2.2}$$

Now we evaluate the field strengths. In the wave zone, where $R_0 \gg c/n\omega$, the non-vanishing spherical components are

$$E_\theta = H_\phi = -\frac{2e\beta}{\pi c R_0}\sin\theta\int_0^\infty nq(\omega)\sin[\omega(t - R_0/c_n)]\,\mathrm{d}\omega. \tag{2.3}$$

The energy flux through the sphere of the radius R_0 is

$$W = R_0^2\int S_r \sin\theta\,\mathrm{d}\theta\,\mathrm{d}\phi \qquad S_r = \frac{c}{4\pi}E_\theta H_\phi.$$

Inserting E_θ and H_ϕ one obtains

$$W = \frac{2e^2\beta^2}{\pi c}\int_0^\infty nJ(\omega)\,\mathrm{d}\omega \qquad J(\omega) = \int_0^\pi q^2\sin\theta\,\mathrm{d}\theta. \tag{2.4}$$

For $\omega t_0 \gg 1$, J can be evaluated in a closed form

$$J = J_{BS} = \frac{1}{\beta^3 n^3}\left(\ln\frac{1+\beta_n}{|1-\beta_n|} - 2\beta_n\right) \qquad \text{for} \quad \beta_n < 1 \tag{2.5}$$

and

$$J = J_{BS} + J_{Ch} \qquad J_{Ch} = \frac{\pi\omega t_0}{\beta_n}\left(1 - \frac{1}{\beta_n^2}\right) \qquad \text{for} \quad \beta_n > 1. \tag{2.6}$$

Tamm identified J_{BS} with the spectral distribution of the bremsstrahlung (BS), arising from instant acceleration and deceleration of the charge at the moments $\pm t_0$, respectively. On the other hand, J_{Ch} was identified with the spectral distribution of the Cherenkov radiation. This is supported by the fact that

$$W_{Ch} = \frac{2e^2\beta^2}{\pi c}\int_0^\infty n J_{Ch}(\omega)\,\mathrm{d}\omega = \frac{2e^2\beta t_0}{c}\int_{\beta_n>1}\omega\,\mathrm{d}\omega\left(1-\frac{1}{\beta_n^2}\right) \tag{2.7}$$

strongly resembles the famous Frank–Tamm formula [11] for an infinite medium obtained in quite a different way.

The main result following from Tamm's formulae is that the energy emitted during the whole charge motion into the solid angle $\mathrm{d}\Omega$, in the frequency interval $\mathrm{d}\omega$ is given by

$$\frac{\mathrm{d}^2\mathcal{E}}{\mathrm{d}\Omega\,\mathrm{d}\omega} = \frac{e^2}{\pi^2 cn}\left[\sin\theta\frac{\sin\omega t_0(1-\beta_n\cos\theta)}{\cos\theta-1/\beta_n}\right]^2. \tag{2.8}$$

This formula is frequently used by experimentalists (see, e.g., [12–14]) for the identification of Cherenkov radiation.

3. Schwinger's approach to Tamm's problem

We begin with the continuity equation following from Maxwell equations:

$$\operatorname{div}\vec{S} + \frac{\partial}{\partial t}\mathcal{E} = -\vec{j}\cdot\vec{E}. \tag{3.1}$$

Here

$$\vec{S} = \frac{c}{4\pi}(\vec{E}\times\vec{H}) \qquad \mathcal{E} = \frac{1}{8\pi}(\epsilon E^2 + \mu H^2).$$

Integrating this equation over the volume V of the sphere S of radius r, surrounding a moving charge, one obtains the following equation describing the energy conservation:

$$\int S_r r^2\,\mathrm{d}\Omega + \frac{\partial}{\partial t}\int\mathcal{E}\,\mathrm{d}V = -\int\vec{j}\cdot\vec{E}\,\mathrm{d}V. \tag{3.2}$$

The usual interpretation of this equation proceeds as follows (see, e.g., [15, pp 276–7]):

> The first term on the left-hand side represents the electromagnetic energy flowing out of the volume V through the surface S_r, and the second term represents the time rate of change of the energy stored by the electromagnetic field within V.

And furthermore:

> The right-hand side, on the other hand, represents the power supplied by the external forces that maintain the charges in dynamic equilibrium.

Schwinger [8] identifies energy losses of a moving charge with the integral on the right-hand side of (3.1)

$$W_S = -\int\vec{j}\cdot\vec{E}\,\mathrm{d}V. \tag{3.3}$$

Substituting $\vec{E} = -\vec{\nabla}\Phi - \dot{\vec{A}}/c$ and integrating by parts, one obtains

$$\begin{aligned} W_S &= -\int\vec{j}\cdot\vec{E}\,\mathrm{d}V = \int\vec{j}\cdot(\vec{\nabla}\Phi + \dot{\vec{A}}/c)\,\mathrm{d}V = -\int(\operatorname{div}\vec{j} - \dot{\vec{A}}/c)\,\mathrm{d}V \\ &= \int(\dot{\rho}\Phi + \dot{\vec{A}}/c)\,\mathrm{d}V = \frac{\mathrm{d}}{\mathrm{d}t}\int\rho\Phi\,\mathrm{d}V - \int(\rho\dot{\Phi} - \dot{\vec{A}}/c)\,\mathrm{d}V. \end{aligned} \tag{3.4}$$

By definition, W_S is the energy lost by a moving charge per unit time. Schwinger discards the first term in the second line of (3.4) on the grounds that 'it is of an accelerated energy type'. The retarded and advanced electromagnetic potentials corresponding to charge current densities ρ and $\vec{j}$ are given by

$$\begin{aligned}\Phi_{ret,adv} &= \frac{1}{\epsilon}\int \frac{1}{R}\rho(\vec{r}',t')\delta(t'-t\pm R/c_n)\,\mathrm{d}V'\,\mathrm{d}t' \\ &= \frac{1}{2\pi\epsilon}\int_{-\infty}^{\infty}\mathrm{d}\omega\,\frac{1}{R}\rho(\vec{r}',t')\exp[\mathrm{i}\omega(t'-t\pm R/c_n)]\,\mathrm{d}V'\,\mathrm{d}t' \\ \vec{A}_{ret,adv} &= \frac{\mu}{c}\int \frac{1}{R}\vec{j}(\vec{r}',t')\delta(t'-t\pm R/c_n)\,\mathrm{d}V'\,\mathrm{d}t' \\ &= \frac{\mu}{2\pi c}\int_{-\infty}^{\infty}\mathrm{d}\omega\frac{1}{R}\vec{j}(\vec{r}',t')\exp[\mathrm{i}\omega(t'-t\pm R/c_n)]\,\mathrm{d}\omega\,\mathrm{d}V'\,\mathrm{d}t'\end{aligned} \tag{3.5}$$

where ϵ and μ are the electric and magnetic permittivities, respectively; $R=|\vec{r}-\vec{r}'|$ and + and − signs refer to retarded and advanced potentials, respectively. Further, Schwinger represents the retarded electromagnetic potentials in the form

$$\begin{aligned}\Phi_{ret} &= \tfrac{1}{2}(\Phi_{ret}+\Phi_{adv})+\tfrac{1}{2}(\Phi_{ret}-\Phi_{adv}) \\ \vec{A}_{ret} &= \tfrac{1}{2}(\vec{A}_{ret}+\vec{A}_{adv})+\tfrac{1}{2}(\vec{A}_{ret}-\vec{A}_{adv})\end{aligned} \tag{3.6}$$

and discards the symmetric part of these equations on the grounds that:

> the first part of (3.3), derived from the symmetrical combination of $\vec{E}_{ret}$ and $\vec{E}_{adv}$, changes sign on reversing the positive sense of time and therefore represents a reactive power. It describes the rate at which the electron stores energy in the electromagnetic field, an inertial effect with which we are not concerned. However, the second part of (3.3), derived from the antisymmetrical combination of $\vec{E}_{ret}$ and $\vec{E}_{adv}$, remains unchanged on reversing the positive sense of time and therefore represents resistive power. Subject to one qualification, it describes the rate of irreversible energy transfer to the electromagnetic field, which is the desired rate of radiation.

Correspondingly, electromagnetic potentials are reduced to

$$\begin{aligned}\Phi &= -\frac{1}{\pi\epsilon}\int_0^{\infty}\mathrm{d}\omega\,\frac{1}{R}\rho(\vec{r}',t')\sin[\omega(t'-t)]\sin(k_nR)\,\mathrm{d}V'\,\mathrm{d}t' \\ \vec{A} &= -\frac{\mu}{\pi c}\int_0^{\infty}\mathrm{d}\omega\,\frac{1}{R}\vec{j}(\vec{r}',t')\sin[\omega(t'-t)]\sin(k_nR/)\,\mathrm{d}V'\,\mathrm{d}t' \qquad k_n=\omega/c_n.\end{aligned} \tag{3.7}$$

Substituting this into (3.4), we obtain

$$W_S=\int_0^{\infty}P(\omega,t)\,\mathrm{d}\omega \tag{3.8}$$

where

$$\begin{aligned}P(\omega,t)=\frac{\mathrm{d}^2E}{\mathrm{d}t\,\mathrm{d}\omega} &= -\frac{\omega}{\pi\epsilon}\int \mathrm{d}V\,\mathrm{d}V'\,\mathrm{d}t'\,\frac{\sin k_nR}{R}\cos\omega(t-t') \\ &\quad\times\left[\rho(\vec{r},t)\rho(\vec{r}',t')-\frac{1}{c_n^2}\vec{j}(\vec{r},t)\cdot\vec{j}(\vec{r}',t')\right]\end{aligned} \tag{3.9}$$

is the energy lost by a moving charge per unit time and per frequency unit. The angular distribution $P(\vec{n},\omega,t)$ is defined as

$$P(\omega,t)=\int P(\vec{n},\omega,t)\,\mathrm{d}\Omega \tag{3.10}$$

where

$$P(\vec{n},\omega,t)=\frac{\mathrm{d}^3E}{\mathrm{d}t\,\mathrm{d}\omega\,\mathrm{d}\Omega}=-\frac{n\omega^2}{4\pi^2c\epsilon}\int \mathrm{d}V\,\mathrm{d}V'\,\mathrm{d}t'\cos\omega\left[(t'-t)+\frac{1}{c_n}\vec{n}(\vec{r}-\vec{r}')\right]$$
$$\times\left[\rho(\vec{r},t)\rho(\vec{r}',t')-\frac{1}{c_n^2}\vec{j}(\vec{r},t)\cdot\vec{j}(\vec{r}',t')\right] \tag{3.11}$$

is the energy lost by a moving charge per unit time, per frequency unit and per unit solid angle. Here $\vec{n}$ is the vector defining the observation point.

Equations (3.9) and (3.11) were obtained by Schwinger [9]. We apply them to the Tamm problem. In what follows we limit ourselves to a dielectric medium for which $\epsilon=n^2$.

3.1. Instant power frequency spectrum

For the treated Tamm problem, charge and current densities are given by

$$j_z=ev\delta(x)\delta(y)\Theta(t+t_0)\Theta(t_0-t)\delta(z-vt)$$
$$\rho(\vec{r},t)=e\delta(x)\delta(y)[\Theta(-t-t_0)\delta(z+z_0) \tag{3.12}$$
$$+\Theta(t+t_0)\Theta(t_0-t)\delta(z-vt)+\Theta(t-t_0)\delta(z-z_0)].$$

Inserting these expressions into (3.9) and performing integrations, one obtains

$$P(\omega,t)=-\frac{\omega e^2}{\pi\epsilon}[\Theta(-t-t_0)P_1+\Theta(t-t_0)P_2+\Theta(t+t_0)\Theta(t_0-t)P_3] \tag{3.13}$$

where

$$P_1=-\frac{\sin\omega(t+t_0)}{c_n}+\frac{\sin 2\omega t_0\beta_n}{2\omega t_0 v}\sin\omega(t-t_0)+\frac{1}{2v}\cos\omega(t+t_0)$$
$$\times\{\mathrm{si}[2\mathrm{t}_0\omega(1+\beta_\mathrm{n})]-\mathrm{si}[2\mathrm{t}_0\omega(1-\beta_\mathrm{n})]\}+\frac{1}{2\mathrm{v}}\sin\omega(\mathrm{t}+\mathrm{t}_0)$$
$$\times\left\{\frac{1}{2}\ln\left(\frac{1+\beta_n}{1-\beta_n}\right)^2+\mathrm{ci}[2\omega\mathrm{t}_0|1-\beta_\mathrm{n}|]-\mathrm{ci}[2\omega\mathrm{t}_0(1+\beta_\mathrm{n})]\right\}$$
$$P_2=\frac{\sin\omega(t-t_0)}{c_n}-\frac{\sin 2\omega t_0\beta_n}{2vt_0\omega}\sin\omega(t+t_0)+\frac{1}{2v}\cos\omega(t-t_0) \tag{3.14}$$
$$\times\{\mathrm{si}[2\mathrm{t}_0\omega(1+\beta_\mathrm{n})]-\mathrm{si}[2\mathrm{t}_0\omega(1-\beta_\mathrm{n})]\}-\frac{1}{2\mathrm{v}}\sin\omega(\mathrm{t}-\mathrm{t}_0)$$
$$\times\left\{\frac{1}{2}\ln\left(\frac{1+\beta_n}{1-\beta_n}\right)^2+\mathrm{ci}[2\omega\mathrm{t}_0|1-\beta_\mathrm{n}|]-\mathrm{ci}[2\omega\mathrm{t}_0\omega(1+\beta_\mathrm{n})]\right\}$$
$$P_3=-\frac{\sin\omega\beta_n(t+t_0)}{v(t+t_0)}\frac{\sin\omega(t+t_0)}{\omega}+\frac{\sin\omega\beta_n(t-t_0)}{v(t-t_0)}\frac{\sin\omega(t-t_0)}{\omega}-\frac{1-\beta_n^2}{2v}$$
$$\times\{\mathrm{si}[(1-\beta_\mathrm{n})\omega(\mathrm{t}_0-\mathrm{t})]-\mathrm{si}[(1+\beta_\mathrm{n})\omega(\mathrm{t}_0-\mathrm{t})]$$
$$+\mathrm{si}[(1-\beta_\mathrm{n})\omega(\mathrm{t}_0+\mathrm{t})]-\mathrm{si}[(1+\beta_\mathrm{n})\omega(\mathrm{t}_0+\mathrm{t})]\}.$$

Here si(x) and ci(x) are the integral sine and cosine. They are defined by the equations

$$\mathrm{si}(\mathrm{x})=-\int_\mathrm{x}^\infty\frac{\sin\mathrm{t}}{\mathrm{t}}\,\mathrm{dt}=-\frac{\pi}{2}+\int_0^\mathrm{x}\frac{\sin\mathrm{t}}{\mathrm{t}}\,\mathrm{dt}=-\frac{\pi}{2}-\sum_{\mathrm{k}=1}^\infty\frac{(-1)^\mathrm{k}}{(2\mathrm{k}-1)(2\mathrm{k}-1)!}\mathrm{x}^{2\mathrm{k}-1}$$

$$\mathrm{ci}(\mathrm{x})=-\int_\mathrm{x}^\infty\frac{\cos\mathrm{t}}{\mathrm{t}}\,\mathrm{dt}=\mathrm{C}+\ln\mathrm{x}-\int_0^\mathrm{x}\frac{1-\cos\mathrm{t}}{\mathrm{t}}\,\mathrm{dt}=\mathrm{C}+\ln\mathrm{x}+\sum_{\mathrm{k}=1}^\infty\frac{(-1)^\mathrm{k}}{2\mathrm{k}(2\mathrm{k})!}\mathrm{x}^{2\mathrm{k}}.$$

Here $C \approx 0.577$ is Euler's constant. For large and small x, si(x) and ci(x) behave as

$$\mathrm{si(x)} \to -\frac{\cos \mathrm{x}}{\mathrm{x}} - \frac{\sin \mathrm{x}}{\mathrm{x}^2} \qquad \mathrm{ci(x)} \to \frac{\sin \mathrm{x}}{\mathrm{x}} - \frac{\cos \mathrm{x}}{\mathrm{x}^2} \qquad \text{for} \quad \mathrm{x} \to +\infty$$

$$\mathrm{si(x)} \to -\pi + \frac{\cos \mathrm{x}}{|\mathrm{x}|} + \frac{\sin |\mathrm{x}|}{\mathrm{x}^2} \qquad \text{for} \quad \mathrm{x} \to -\infty$$

$$\mathrm{si(x)} \to -\tfrac{1}{2}\pi + \mathrm{x} \qquad \mathrm{ci(x)} \to \mathrm{C} + \ln \mathrm{x} - \tfrac{1}{4}\mathrm{x}^2 \qquad \text{for} \quad \mathrm{x} \to 0.$$

The following relations

$$\int_0^x \frac{\sin^2 t}{t}\,\mathrm{d}t = \tfrac{1}{2}C + \tfrac{1}{2}\ln 2|x| - \tfrac{1}{2}\mathrm{ci}(2|\mathrm{x}|) \qquad \mathrm{si(x)} + \mathrm{si}(-\mathrm{x}) = -\pi$$

will also be useful.

The non-vanishing of P_1 and P_2 terms in (3.13) is due to the fact that Fourier transforms of a static charge density corresponding to charge at rest prior to the beginning of the charge motion ($t < -t_0$) and after its termination ($t > t_0$) contribute to (3.9) and (3.11). To see this explicitly, we write out the Fourier transform of charge density (3.12):

$$\begin{aligned}\rho(\vec{r},\omega) &= \frac{1}{2\pi}\int_{-\infty}^{\infty} \exp(-\mathrm{i}\omega t)\rho(\vec{r},t)\,\mathrm{d}t \\ &= \frac{1}{2\pi}e\delta(x)\delta(y)[\delta(z+z_0)\int_{-\infty}^{-t_0}\exp(-\mathrm{i}\omega t)\,\mathrm{d}t + \delta(z-z_0)\int_{t_0}^{\infty}\exp(-\mathrm{i}\omega t)\,\mathrm{d}t \\ &\quad + \frac{1}{v}\Theta(z+z_0)\Theta(z_0-z)\exp(-\mathrm{i}\omega z/v)].\end{aligned}$$

The first term on the right-hand side corresponds to the charge which rests at the point $z = -z_0$ up to a moment $t = -t_0$; the second term on the right-hand side corresponds to the charge which rests at the point $z = z_0$ after the moment $t = t_0$. Finally, the third term corresponds to the charge moving between $-z_0$ and z_0 points in the time interval $-t_0 < t < t_0$. It should be noted that the first and second terms in this expression are Fourier densities of a charge which does not permanently rest at the points $z = \pm z_0$, but up to a moment $-t_0$ and after the moment t_0, respectively. In fact, the Fourier density corresponding to a charge which is permanently at rest at the point $z = z_0$ is

$$\frac{e}{2\pi}\delta(z-z_0)\int_{-\infty}^{\infty}\exp(\mathrm{i}\omega t)\,\mathrm{d}t = e\delta(z-z_0)\delta(\omega).$$

In the limit $\omega t_0 \to \infty$, equations (3.14) pass into

$$P_1 = -\frac{1}{c_n}\sin[\omega(t+t_0)]\left(1 - \frac{1}{2\beta_n}\ln\frac{1+\beta_n}{1-\beta_n}\right)$$

$$P_2 = +\frac{1}{c_n}\sin[\omega(t-t_0)]\left(1 - \frac{1}{2\beta_n}\ln\frac{1+\beta_n}{1-\beta_n}\right) \qquad P_3 = 0$$

for $\beta_n < 1$ and

$$\begin{aligned}P_1 &= -\frac{1}{c_n}\sin[\omega(t+t_0)]\left(1 - \frac{1}{2\beta_n}\ln\frac{1+\beta_n}{\beta_n-1}\right) + \frac{\pi}{2v}\cos\omega\left(t+\frac{z_0}{v}\right) \\ P_2 &= \frac{1}{c_n}\sin[\omega(t-t_0)]\left(1 - \frac{1}{2\beta_n}\ln\frac{1+\beta_n}{\beta_n-1}\right) + \frac{\pi}{2v}\cos\omega\left(t-\frac{z_0}{v}\right) \qquad (3.15) \\ P_3 &= -\frac{\pi}{v}(\beta_n^2-1)\end{aligned}$$

for $\beta_n > 1$. It is seen that the energy radiated for the time interval $-t_1 < t < t_1, t_1 < t_0$ equals zero for $\beta_n < 1$ and equals $2\omega v e^2 t_1(1 - 1/\beta_n^2)/c^2$ for $\beta_n > 1$. This coincides exactly with the Cherenkov radiation spectrum for unbounded charge motion (see, e.g., Frank's book [11]). It should be noted that expressions for P_3 in (3.15) were obtained under the assumption that the arguments of si and ci of P_3 entering into (3.14) are sufficiently large, that is, there should be $\omega(t_0 - t) \gg 1$. This means that P_3 in (3.15) are valid if the observation moment t is not too close to t_0.

On the other hand, the terms P_1 and P_2 in (3.15) were obtained without this assumption. In particular, the term P_2 different from zero for $t > t_0$ shows how the bremsstrahlung and Cherenkov radiation behave for $t > t_0$, i.e. after termination of charge motion. Since the part of P_2

$$\frac{1}{c_n} \sin\left[\omega\left(t - \frac{z_0}{v}\right)\right]\left(1 - \frac{1}{2\beta_n} \ln \frac{\beta_n + 1}{|\beta_n - 1|}\right)$$

is present both for $\beta_n < 1$ and $\beta_n > 1$, it may be associated with BS. On the other hand, the part of P_2

$$\frac{\pi}{2v} \cos\left[\omega\left(t - \frac{z_0}{v}\right)\right]$$

that differs from zero only for $\beta_n > 1$ may be conditionally attributed to the Cherenkov post-action.

We observe that for $t < -t_0$ and $t > t_0$, the radiation intensity is a rapidly oscillating function of time t. The time average of this intensity is zero, so it could hardly be observed experimentally. Since, on the other hand, for $\beta_n > 1$, the radiation intensity does not depend on time in the time interval $-t_1 < t < t_1$, $t_1 \ll t_0$, it contributes coherently to the radiated energy.

To obtain the energy radiated for a finite time interval, one should integrate (3.13) over t. However, the integrals that arise involve integral sine and cosine functions. Since we did not succeed in evaluating these integrals in a closed form, we follow an indirect method in the following sections. In section 3.2, we evaluate the instant angular-frequency distribution of the radiated energy. Integrating it over time we obtain (section 3.3) the angular-frequency distribution of the energy radiated for a finite time interval. Finally, integrating the latter over angular variables we obtain a closed expression for the frequency distribution of the energy radiated for a finite time interval (section 3.4).

3.2. Instant angular-frequency distribution of the power spectrum

Due to the axial symmetry of the problem, $\vec{n} \cdot (\vec{r} - \vec{r}') = \cos\theta(z - z')$ in the integrand in (3.11), where θ is the inclination angle of $\vec{n}$ towards the motion axis. Integration over the spacetime variables in (3.11) gives

$$P(\vec{n}, \omega, t) = \frac{\mathrm{d}^3\mathcal{E}}{\mathrm{d}t\, \mathrm{d}\omega\, \mathrm{d}\Omega} = -\frac{\omega e^2 \beta}{2\pi^2 c} \frac{\sin[\omega t_0(1 - \beta_n \cos\theta)]}{1 - \beta_n \cos\theta}$$
$$\times[\Theta(-t - t_0)P_{1n} + \Theta(t - t_0)P_{2n} + \Theta(t + t_0)\Theta(t_0 - t)P_{3n}]. \tag{3.16}$$

Here

$$P_{1n} = \cos\theta \cos[\omega(t + t_0\beta_n \cos\theta)]$$
$$P_{2n} = \cos\theta \cos[\omega(t - t_0\beta_n \cos\theta)]$$
$$P_{3n} = (\cos\theta - \beta_n) \cos[\omega t(1 - \beta_n \cos\theta)].$$

3.3. Angular-frequency distribution of the radiated energy for a finite time interval

Integrating (3.16) over the time interval $-t_1 < t < t_1$, $t_1 < t_0$, one obtains the Fourier distribution of the energy detected for a time $2t_1$ radiated by a particle moving in the time interval $2t_0$, $t_1 < t_0$:

$$\mathcal{E}(\vec{n},\omega,t_1) = \int_{-t_1}^{t_1} P(\vec{n},\omega,t)\,\mathrm{d}t$$
$$= \frac{e^2\beta}{\pi^2 c}(\beta_n - \cos\theta)\frac{\sin\omega t_0(1-\beta_n\cos\theta)}{1-\beta_n\cos\theta}\frac{\sin\omega t_1(1-\beta_n\cos\theta)}{1-\beta_n\cos\theta}. \tag{3.17}$$

Let $\omega t_0 \to \infty$. Then,

$$\mathcal{E}(\vec{n},\omega,t_1) \to \frac{e^2\beta\omega t_1}{\pi c}\left(1-\frac{1}{\beta_n^2}\right)\delta\left(\cos\theta - \frac{1}{\beta_n}\right). \tag{3.18}$$

This coincides with the angular-frequency distribution of the radiated energy in Tamm–Frank theory [11] describing the unbounded charge motion. For $\cos\theta = 1/\beta_n$ equation (3.17) reduces to

$$\mathcal{E}(\vec{n},\omega,t_1) = \frac{e^2}{\pi n c}(\beta_n^2 - 1)\omega^2 t_0 t_1.$$

It vanishes for $\beta_n = 1$.

Let $t_1 > t_0$. Then,

$$\mathcal{E}(\vec{n},\omega,t_1) = \frac{e^2\beta}{\pi^2 c}\frac{\sin[\omega t_0(1-\beta_n\cos\theta)]}{1-\beta_n\cos\theta}$$
$$\times\left[\beta_n\sin^2\theta\frac{\sin\omega t_0(1-\beta_n\cos\theta)}{1-\beta_n\cos\theta} - \cos\theta\sin\omega(t_1 - t_0\beta_n\cos\theta)\right] \tag{3.19}$$

is the angular-frequency distribution of the energy detected for the time interval $2t_1 > 2t_0$. The first term in square brackets coincides with Tamm's angular distribution (2.8). The second term originating from integration of P_1 and P_2 terms in (3.16) describes the boundary effects. The physical reason for the appearance of the extra term in (3.19) (the second term in square brackets) is due to the following reason. The magnetic field $\vec{H}$ is defined as the curl of VP (2.2). Tamm obtained the electric field from the Maxwell equation

$$\mathrm{curl}\,\vec{H} = \frac{\epsilon}{c}\frac{\partial\vec{E}}{\partial t}$$

valid outside the motion interval. In the ω representation this equation looks like

$$\mathrm{curl}\,\vec{H}_\omega = \frac{\mathrm{i}\omega\epsilon}{c}\vec{E}_\omega.$$

This equation suggests that the contribution of the static electric field existing before the beginning of the charge motion and after its termination has dropped from Tamm's formulae given in section 2 (because VP (2.1) and the magnetic field (2.3) describe only the motion of charge on the interval $(-z_0, z_0)$). On the other hand, Schwinger's equations (3.9) and (3.11) contain the static electric field contributions of a charge which is at rest up to the moment $t = -t_0$ and after the moment $t = t_0$. They are responsible for the appearance of an extra term in (3.19). In the $\vec{r}, t$ representation, the contribution of the static electromagnetic field strengths is not essential in the wave zone.

Taking into account that

$$\frac{\sin\alpha x}{x} \to \pi\delta(x) \qquad \text{and} \qquad \frac{1}{\alpha}\left[\frac{\sin\alpha x}{x}\right]^2 \to \pi\delta(x) \qquad \text{for} \quad \alpha \to \infty \tag{3.20}$$

one obtains from (3.19) for large ωt_0

$$\mathcal{E}(\vec{n},\omega,t_1) = \frac{e^2}{\pi cn}\delta(1-\beta_n\cos\theta)\left[\omega t_0(\beta_n^2-1) - \sin\omega\left(t_1 - \frac{z_0}{v}\right)\right]. \tag{3.21}$$

For $\beta_n \neq 1$, the second term inside the square brackets may be discarded, and one obtains

$$\mathcal{E}(\vec{n},\omega,t_1) = \frac{e^2}{\pi cn}\omega t_0(\beta_n^2-1)\delta(1-\beta_n\cos\theta). \tag{3.22}$$

For $\cos\theta = 1/\beta_n$, equation (3.19) is reduced to

$$\mathcal{E}(\vec{n},\omega,t_1) = \frac{e^2}{\pi nc}(\beta_n^2-1)\omega^2 t_0^2 - \frac{e^2}{\pi nc}\omega t_0 \sin\omega(t_1-t_0).$$

It does not vanish at $\beta_n = 1$.

Equations (3.17) and (3.19) generalize Tamm's angular-frequency distribution (2.8) for $t_1 \neq t_0$.

3.4. Frequency distribution of the radiated energy

Integrating (3.17) over the solid angle one finds the following expression for the frequency distribution of the radiated power for the case when the detection time $2t_1$ is smaller than the motion time $2t_0$:

$$\begin{aligned}\mathcal{E}(\omega,t_1) = \frac{e^2\beta}{\pi c}\left(1-\frac{1}{\beta_n^2}\right)\Bigg\{&\frac{\cos(\omega(t_1-t_0)(1-\beta_n))}{1-\beta_n} - \frac{\cos(\omega(t_0-t_1)(1+\beta_n))}{1+\beta_n}\\ &-\frac{\cos(\omega(t_1+t_0)(1-\beta_n))}{1-\beta_n} + \frac{\cos(\omega(t_1+t_0)(1+\beta_n))}{1+\beta_n}\\ &+\omega(t_0-t_1)[\mathrm{si}(\omega(\mathrm{t_0}-\mathrm{t_1})(1-\beta_\mathrm{n})) - \mathrm{si}(\omega(\mathrm{t_0}-\mathrm{t_1})(1+\beta_\mathrm{n}))]\\ &-\omega(t_0+t_1)[\mathrm{si}(\omega(\mathrm{t_0}+\mathrm{t_1})(1-\beta_\mathrm{n})) - \mathrm{si}(\omega(\mathrm{t_0}+\mathrm{t_1})(1+\beta_\mathrm{n}))]\Bigg\}\\ &-\frac{e^2}{\pi\epsilon v}[\mathrm{ci}(\omega(\mathrm{t_0}-\mathrm{t_1})|1-\beta_\mathrm{n}|) - \mathrm{ci}(\omega(\mathrm{t_0}-\mathrm{t_1})(1+\beta_\mathrm{n}))\\ &-\mathrm{ci}(\omega(\mathrm{t_0}+\mathrm{t_1})|1-\beta_\mathrm{n}|) + \mathrm{ci}(\omega(\mathrm{t_0}+\mathrm{t_1})(1+\beta_\mathrm{n}))].\end{aligned} \tag{3.23}$$

Now let $t_1 > t_0$ (i.e. the detection time is greater than the motion time). Then,

$$\mathcal{E}(\omega,t_1) = \frac{2e^2\beta}{\pi c}(\beta_n I_1 - I_2) \tag{3.24}$$

where

$$I_1 = \int \sin^3\theta\,\mathrm{d}\theta\left[\frac{\sin\omega t_0(1-\beta_n\cos\theta)}{1-\beta_n\cos\theta}\right]^2$$

$$= \frac{1}{\beta_n}\left(1-\frac{1}{\beta_n^2}\right)\left\{\frac{\sin^2\omega t_0(1-\beta_n)}{1-\beta_n} - \frac{\sin^2\omega t_0(1+\beta_n)}{1+\beta_n}\right.$$

$$\left.-\omega t_0[\mathrm{si}(2\omega\mathrm{t}_0(1-\beta_\mathrm{n})) - \mathrm{si}(2\omega\mathrm{t}_0(1+\beta_\mathrm{n}))]\right\}$$

$$-\frac{1}{\beta_n^3}\left[\ln\frac{|1-\beta_n|}{1+\beta_n} - \mathrm{ci}(2\omega\mathrm{t}_0|1-\beta_\mathrm{n}|) + \mathrm{ci}(2\omega\mathrm{t}_0(1+\beta_\mathrm{n}))\right]$$

$$-\frac{1}{\beta_n^2} - \frac{1}{4\beta_n^3\omega t_0}[\sin(2\omega t_0(1-\beta_n)) - \sin(2\omega t_0(1+\beta_n))]$$

$$I_2 = \int \sin\theta\cos\theta\,\mathrm{d}\theta\,\frac{\sin\omega t_0(1-\beta_n\cos\theta)\sin\omega(t_1-t_0\beta_n\cos\theta)}{1-\beta_n\cos\theta}$$

$$= -\frac{1}{4\beta_n^2\omega t_0}\sin\omega(t_1-t_0)[\cos(2\omega t_0(1-\beta_n)) - \cos(2\omega t_0(1+\beta_n))]$$

$$-\frac{1}{\beta_n}\cos\omega(t_1-t_0) - \frac{1}{4\beta_n^2\omega t_0}\cos\omega(t_1-t_0)$$

$$\times[\sin(2\omega t_0(1-\beta_n)) - \sin(2\omega t_0(1+\beta_n))]$$

$$-\frac{1}{2\beta_n^2}\sin\omega(t_1-t_0)[\mathrm{si}(2\omega\mathrm{t}_0(1-\beta_\mathrm{n})) - \mathrm{si}(2\omega\mathrm{t}_0(1+\beta_\mathrm{n}))]$$

$$-\frac{1}{2\beta_n^2}\cos\omega(t_1-t_0)\left[\ln\frac{|1-\beta_n|}{1+\beta_n} - \mathrm{ci}(2\omega\mathrm{t}_0|1-\beta_\mathrm{n}|) + \mathrm{ci}(2\omega\mathrm{t}_0(1+\beta_\mathrm{n}))\right].$$

The typical dependence of $\mathcal{E}$ on t_0 for t_1 fixed is shown in figure 1. For large ωt_0 and $\beta_n < 1$, it oscillates around the zero value. For large ωt_0 and $\beta_n > 1$, $\mathcal{E}$ oscillates around the value

$$\frac{2e^2\omega t_1\beta}{c}\left(1-\frac{1}{\beta_n^2}\right)$$

given by the Tamm–Frank theory [11]. In both cases the amplitude of oscillations decreases as $1/\omega t_0$ for large t_0.

The typical dependence of $\mathcal{E}$ on t_1 for t_0 fixed is shown in figure 2. Since I_2 is a periodic function of t_1 and I_1 does not depend on t_0, $\mathcal{E}$ oscillates around the value $2e^2\beta^2 n I_1/\pi c$. Previously, the frequency distribution of the radiated energy within the framework of Tamm's theory was given by Kobzev and Frank [16] and by Kobzev *et al* [17]. It is obtained by integrating (2.8) over the angular variables:

$$\frac{\mathrm{d}\mathcal{E}}{\mathrm{d}\omega} = \frac{2e^2\beta}{\pi c}\left(1-\frac{1}{\beta_n^2}\right)\left\{\frac{\sin^2\omega t_0(1-\beta_n)}{1-\beta_n} - \frac{\sin^2\omega t_0(1+\beta_n)}{1+\beta_n}\right.$$

$$\left.-\omega t_0[\mathrm{si}(2\omega\mathrm{t}_0(1-\beta_\mathrm{n})) - \mathrm{si}(2\omega\mathrm{t}_0(1+\beta_\mathrm{n}))]\right\}$$

$$-\frac{2e^2}{\pi cn\beta_n}\left[\ln\frac{|1-\beta_n|}{1+\beta_n} - \mathrm{ci}(2\omega\mathrm{t}_0|1-\beta_\mathrm{n}|) + \mathrm{ci}(2\omega\mathrm{t}_0(1+\beta_\mathrm{n}))\right]$$

$$-\frac{e^2}{\pi cn\beta_n}\left\{2\beta_n + \frac{1}{2\omega t_0}[\sin 2\omega t_0(1-\beta_n)) - \sin 2\omega t_0(1+\beta_n))]\right\}. \qquad (3.25)$$

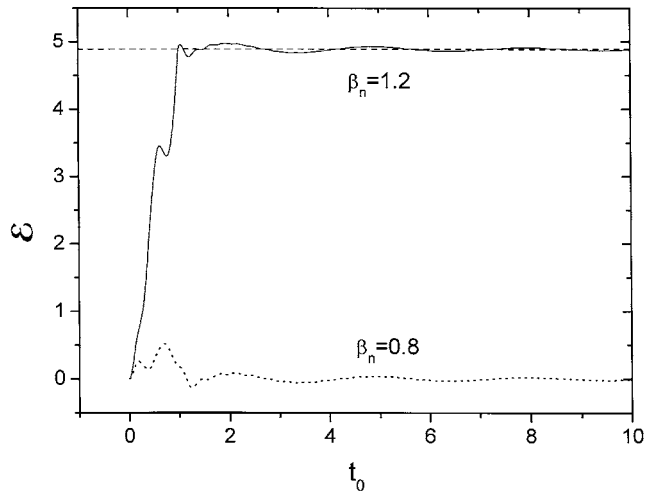

Figure 1. Energy $\mathcal{E}$ detected in a fixed time interval t_1 as a function of charge motion time t_0. For $\beta_n < 1$, $\mathcal{E}$ oscillates around zero. For $\beta_n > 1$ it oscillates around the finite value (3.25). The amplitude of oscillations decreases as $1/\omega t_0$ for large motion time t_0. $\mathcal{E}$ is given in units of e^2/c and t_0 in units of t_1.

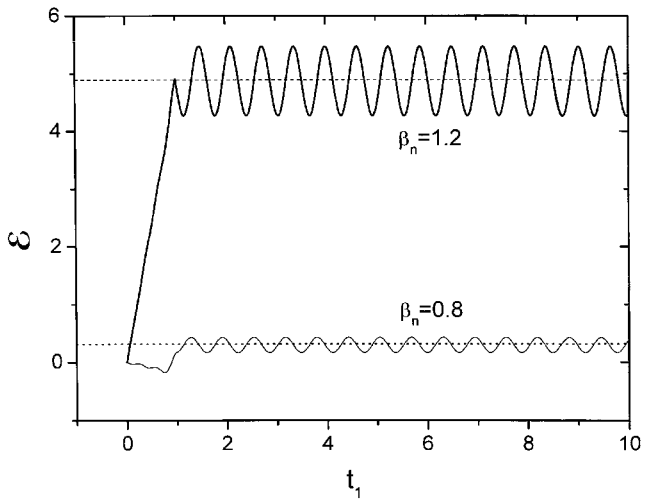

Figure 2. Energy $\mathcal{E}$ as a function of the detection time t_1 for the fixed motion time t_0. The time motion interval t_0 is fixed. For $\beta_n < 1$ and $\beta_n > 1$, $\mathcal{E}$ oscillates around the Tamm's values (2.5) and (2.6), respectively. Contrary to the previous figure, there is no damping of oscillations. $\mathcal{E}$ is given in units of e^2/c; t_1, in units of t_0.

This expression coincides with the first term in (3.24) which involves I_1. For large ωt_0, equation (3.25) turns into Tamm's equations (2.5) and (2.6).

The frequency dependences of the energy radiated for time t_1 are shown in figures 3 and 4. In figure 3, one sees the frequency dependence for the case when the observation time $2t_1$ is twice as small as the charge motion time $2t_0$. For $\beta_n < 1$, the radiated energy is concentrated

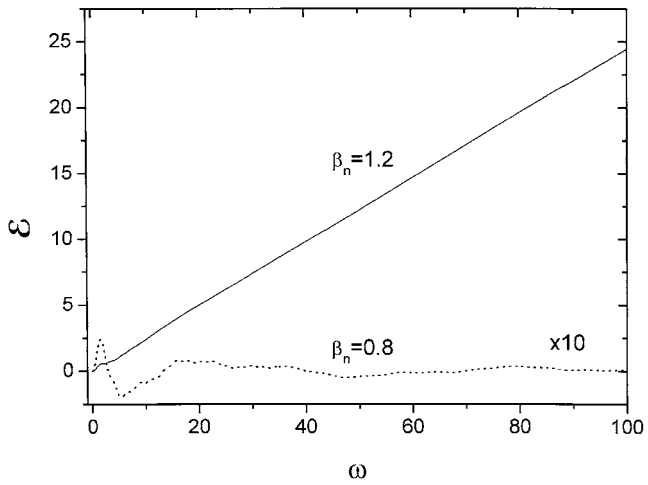

Figure 3. Frequency dependence of the radiated energy for $t_1/t_0 = 0.5$. $\mathcal{E}$ is given in units of e^2/c and ω in units of $1/t_0$.

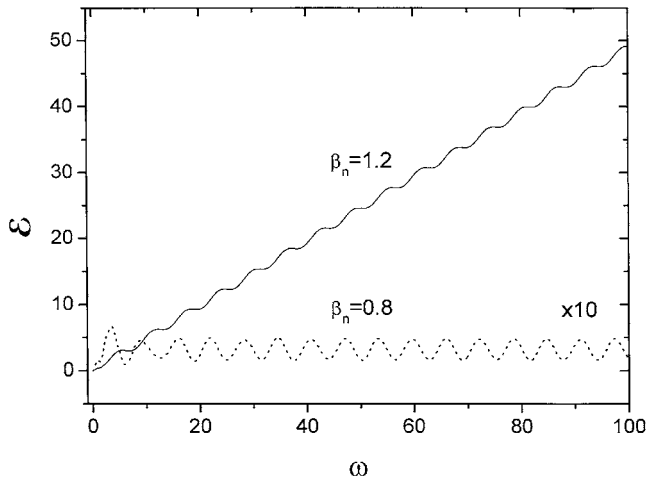

Figure 4. Frequency dependence of the radiated energy for $t_1/t_0 = 2$. $\mathcal{E}$ is given in units of e^2/c and ω in units of $1/t_0$.

near zero, while for $\beta_n > 1$ it rises linearly with frequency

$$\mathcal{E} \sim \frac{2e^2\omega t_1\beta_n}{cn}\left(1 - \frac{1}{\beta_n^2}\right).$$

The frequency dependence for the case when the observation time $2t_1$ is twice the charge motion time $2t_0$ is shown in figure 4. For $\beta_n < 1$, the radiated energy oscillates around Tamm's value

$$\frac{4e^2}{\pi cn}\left(\ln\frac{1+\beta_n}{1-\beta_n} - 1\right)$$

while for $\beta_n > 1$, it again rises linearly, but with a coefficient different from the $t_1 < t_0$ case:

$$\mathcal{E} \sim \frac{2e^2\omega t_0\beta}{c}\left(1 - \frac{1}{\beta_n^2}\right).$$

3.4.1. Large interval motion. Let the observation time be less than the motion time ($t_1 < t_0$). Then, for $\omega(t_0 - t_1) \gg 1$, $\mathcal{E}(\omega, t_1)$ is very small for $\beta_n < 1$. On the other hand, for $\beta_n > 1$,

$$\mathcal{E}(\omega, t_1) = \frac{2\omega t_1 e^2 \beta}{c}\left(1 - \frac{1}{\beta_n^2}\right). \tag{3.26}$$

This coincides with the frequency distribution of the radiated energy over the whole charge motion in Frank–Tamm theory.

Now let the observation time be greater than the motion time ($t_1 > t_0$). Then, for $\omega t_0 \gg 1$ (but $t_1 > t_0$), one obtains

$$\mathcal{E}(\omega, t_1) \approx -\frac{2e^2}{\pi cn}[2 - \cos\omega(t_1 - t_0)]\left(1 + \frac{1}{2\beta_n}\ln\frac{1-\beta_n}{1+\beta_n}\right) \tag{3.27}$$

for $\beta_n < 1$ and

$$\mathcal{E}(\omega, t_1) \approx \frac{2e^2\beta}{\pi c}\left\{\pi\omega t_0\left(1 - \frac{1}{\beta_n^2}\right)\right.$$
$$\left. -\frac{1}{\beta_n}[2 - \cos\omega(t_1 - t_0)]\left(1 + \frac{1}{2\beta_n}\ln\frac{\beta_n - 1}{1+\beta_n}\right) - \frac{\pi}{2\beta_n^2}\sin\omega(t_1 - t_0)\right\} \tag{3.28}$$

for $\beta_n > 1$.

The non-oscillating parts of these expressions coincide with equations (2.5) given by Tamm. According to his own words, equations (2.5) 'are obtained by neglecting the fast-oscillating terms of the form $\sin\omega t_0$' (Tamm gives only equations (2.5) and (2.6) without deriving them). On the other hand, equation (3.25) obtained in [16, 17] gives in the limit $\omega t_0 \to \infty$ to Tamm's expressions (2.5) with additional oscillating terms decreasing as $1/\omega t_0$.

Since some terms in (3.23) and (3.24) depend on $(1 - \beta_n)(t_0 - t_1)$ and $(1 - \beta_n)(t_0 + t_1)$ parameters, equations (3.26)–(3.28) are not valid for $\beta_n \sim 1$ (this corresponds to Cherenkov's threshold).

3.4.2. Frequency distribution on the Cherenkov threshold. Thus, the case $\beta_n = 1$ needs special consideration. One obtains

$$\mathcal{E}(\omega, t_1) = -\frac{e^2}{\pi nc}\left[\ln\frac{t_0 - t_1}{t_0 + t_1} - \mathrm{ci}(2\omega(\mathrm{t_0} - \mathrm{t_1})) + \mathrm{ci}(2\omega(\mathrm{t_0} + \mathrm{t_1}))\right] \tag{3.29}$$

for $t_1 < t_0$. This expression tends to zero for t_1 fixed and $t_0 \to \infty$.

On the other hand, for $t_1 > t_0$

$$\mathcal{E}(\omega, t_1) = \frac{2e^2}{\pi nc}\left\{[1 - \tfrac{1}{2}\cos\omega(t_1 - t_0)][C + \ln(4\omega t_0) - \mathrm{ci}(4\omega \mathrm{t_0})]\right.$$
$$-[1 - \cos\omega(t_1 - t_0)]\left[1 - \frac{\sin(4\omega t_0)}{4\omega t_0}\right]$$
$$\left. +\sin\omega(t_1 - t_0)\left[\frac{1 - \cos(4\omega t_0)}{4\omega t_0} - \frac{\pi}{4} - \frac{1}{2}\sin(4\omega t_0)\right]\right\}. \tag{3.30}$$

The non-oscillating part of this expression coincides with that given by Tamm [1]:

$$\mathcal{E}_T = \frac{2e^2}{\pi nc}[C + \ln(4\omega t_0) - 1].$$

On the other hand, equation (3.27) obtained by Kobzev and Frank for $\beta_n = 1$ goes into

$$\mathcal{E}_{KF} = \frac{2e^2}{\pi nc}\left[C + \ln(4\omega t_0) - 1 - \mathrm{ci}(4\omega \mathrm{t}_0) + \frac{\sin(4\omega \mathrm{t}_0)}{4\omega \mathrm{t}_0}\right].$$

For $(t_1 - t_0)$ fixed and $t_0 \to \infty$, equation (3.30) is reduced to

$$\mathcal{E}(\omega, t_1) \to \frac{2e^2}{\pi nc}\left\{[1 - \tfrac{1}{2}\cos\omega(t_1 - t_0)][C + \ln(4\omega t_0)]\right.$$
$$\left. -1 + \cos\omega(t_1 - t_0) - \sin\omega(t_1 - t_0)\left[\tfrac{1}{4}\pi + \tfrac{1}{2}\sin(4\omega t_0)\right]\right\}. \tag{3.31}$$

In the limit $t_0 \to \infty$, $\mathcal{E}_{KF}$ turns into $\mathcal{E}_T$ plus oscillating terms decreasing as $1/\omega t_0$. On the other hand, the main result of section 3 is that Schwinger's approach incorporates both Tamm–Frank and Tamm problems. Tamm and Frank's results are obtained when the observation time t_1 is smaller than the charge motion time t_0 and $t_0 \to \infty$. In particular, there is no radiation in the non-dispersive medium when the charge velocity is smaller than the velocity of light in the medium. The radiated energy rises in direct proportion to the observation time t_1 for $\beta_n > 1$. Tamm's problem is obtained when $t_1 > t_0$ and t_0 (and, therefore, t_1) tends to ∞. The intensity oscillates around Tamm's value for $\beta_n < 1$ and rises in proportion to the time of charge motion t_0 for $\beta_n > 1$.

4. Exact electromagnetic fields in Tamm's problem

Tamm's energy flux (2.8) radiated during the whole charge motion into the solid angle $\mathrm{d}\Omega$ in the frequency range $\mathrm{d}\omega$ is widely used by experimentalists for identification of the Cherenkov radiation. The aim of this section is to compare (2.8) with the energy flux obtained by exact solution of Tamm's problem.

However, first, we elucidate which approximations were made during the transition from the exact vector potential (2.1) to Tamm's formula (2.8):

(a) Changing R by R_0 outside the exponent means that the observation is made on the sphere with radius R_0 much larger than the motion interval z_0, i.e.

$$R_0 \gg z_0. \tag{4.1}$$

(b) Tamm's field strengths (2.3) are valid only in the wave zone where

$$\omega R_0/c_n \gg 1. \tag{4.2}$$

(c) When changing R under the sign of the exponent in (2.1) by $R_0 - z'\cos\theta$, it is implicitly assumed that the quadratic term in the expansion of R is small compared with the linear one. Consider this more carefully. We expand R up to the second order:

$$R \approx R_0 - z'\cos\theta + \frac{z'^2}{2R_0}\sin^2\theta.$$

Under the sign of the exponent in (2.1), the following terms appear:

$$\frac{z'}{v} + \frac{1}{c_n}\left(R_0 - z'\cos\theta + \frac{z'^2}{2R_0}\sin^2\theta\right).$$

We collect terms involving z'

$$\frac{z'}{c_n}\left[\left(\frac{1}{\beta_n} - \cos\theta\right) + \frac{z'}{2R_0}\sin^2\theta\right].$$

Taking for z' its maximal value z_0, we present the condition for the second term in the expansion of R to be small in the form [7]

$$z_0 \ll 2R_0\left(\frac{1}{\beta_n} - \cos\theta\right)\Big/ \sin^2\theta. \tag{4.3}$$

It is seen that the right-hand side of this equation vanishes for $\cos\theta = 1/\beta_n$, i.e. at the angle where the Cherenkov radiation exists. Therefore, in this angular region the second-order terms may be important.

(d) Under the sign of the exponent in (2.1) the second-order term should be small compared with π, i.e. the inequality

$$\frac{z'^2\omega\sin^2\theta}{2R_0c_n} \ll \pi \tag{4.4}$$

should hold. Or, taking for θ and z' their maximal values ($\theta = \pi/2$, $z' = z_0$), one obtains [11]

$$\frac{z_0^2\omega}{2R_0c_n} \ll \pi. \tag{4.5}$$

From (4.2) and (4.5) one finds the following restriction on ω:

$$\frac{c_n}{R_0} \ll \omega \ll \frac{2\pi R_0c_n}{z_0^2}. \tag{4.6}$$

In the λ language ($\omega = 2\pi c/\lambda$) this condition looks like

$$\frac{nz_0^2}{R_0} \ll \lambda \ll 2\pi nR_0. \tag{4.7}$$

Let $\lambda = 4\times10^{-5}$ cm (the middle of the optical region), $n = 1.5$ (glass). For the typical value $R = 100$ cm, the right-hand side of the inequality (4.7) is fulfilled to a great degree of accuracy. Then the left-hand side of (4.7) gives $z_0 \ll 5\times10^{-2}$ cm. On the other hand, z_0 should not be too small. In fact, for $k_nz_0 \ll 1$, Tamm's formula (2.8) is reduced to

$$\frac{\mathrm{d}^2\mathcal{E}}{\mathrm{d}\omega\,\mathrm{d}\Omega} \sim \frac{e^2\sin^2\theta\omega^2t_0^2}{\pi^2cn\beta_n^2}$$

i.e. the Cherenkov diffraction picture disappears. Therefore, the width interval $10^{-4} < z_0 < 10^{-2}$ cm turns out to be optimal for the validity of Tamm's formula and the existence of the pronounced Cherenkov maximum in the treated case.

It should be noted that for gases, these restrictions are less restrictive than for solids and liquids. In fact, since for them $\beta_n \approx 1$, one obtains

$$\left(\frac{1}{\beta_n} - \cos\theta\right)\Big/ \sin^2\theta \approx \frac{1-\cos\theta}{\sin^2\theta} = 1/2\cos^2(\theta/2).$$

Since for gases the angular spectrum is confined to the $\theta \approx 0$ region, equation (4.3) is reduced to (4.1). The same is true for equation (4.4). As a result, for gases, Tamm's expression (2.8) for the radiated power works when equations (4.1) and (4.2) are fulfilled.

Conditions (4.1)–(4.7) ensuing the validity of Tamm's expressions are spread over different sources. We collected them together to make the interpretation of the numerical results given below easier.

The radial energy flux through the unit solid angle of sphere of the radius R_0 for the whole time of charge motion is given by

$$\frac{\mathrm{d}W}{\mathrm{d}\Omega} = \frac{c}{4\pi} R_0^2 \int_{-\infty}^{\infty} \mathrm{d}t\,(\vec{E} \times \vec{H})_r \,\mathrm{d}\Omega. \tag{4.8}$$

Expressing $\vec{E}$ and $\vec{H}$ through their Fourier transforms

$$\vec{E} = \int \exp(\mathrm{i}\omega t)\vec{E}_\omega \,\mathrm{d}\omega \qquad \vec{H} = \int \exp(\mathrm{i}\omega t)\vec{H}_\omega \,\mathrm{d}\omega$$

and integrating over t, one obtains

$$\frac{\mathrm{d}W}{\mathrm{d}\Omega} = \frac{cR_0^2}{2} \int_{-\infty}^{\infty} (\vec{E}(\omega) \times \vec{H}(-\omega))\,\mathrm{d}\omega = \int_0^{\infty} S(\omega)\,\mathrm{d}\omega \tag{4.9}$$

where

$$S(\omega) = \frac{\mathrm{d}^2 W}{\mathrm{d}\omega\,\mathrm{d}\Omega} = cR_0^2\big[\vec{E}_\theta^{(r)}(\omega)\vec{H}_\phi^{(r)}(\omega) + \vec{E}_\theta^{(i)}(\omega)\vec{H}_\phi^{(i)}(\omega)\big]. \tag{4.10}$$

This quantity shows how the Fourier component of the energy radiated for the whole time of charge motion is distributed over the sphere S. It does not depend on time. The superscripts (r) and (i) mean the real and imaginary parts of E_θ and H_ϕ. Exact field strengths obtained by differentiation of the exact vector potential (2.1) are given by

$$\begin{aligned}
H_\phi^{(r)} &= \frac{ek_n z_0}{2\pi c R_0} \sin\theta \int \frac{G}{R^2}\,\mathrm{d}z' \qquad H_\phi^{(i)} = \frac{ek_n z_0}{2\pi c R_0} \sin\theta \int \frac{F}{R^2}\,\mathrm{d}z' \\
E_\theta^{(r)} &= \frac{ek_n^2 z_0}{2\pi\omega\epsilon R_0} \sin\theta \left(\int \frac{1 - z'\epsilon_0 \cos\theta}{R^3} F_1\,\mathrm{d}z' - \frac{2}{k_n R_0} \int \frac{F}{R^2}\,\mathrm{d}z' \right) \\
E_\theta^{(i)} &= \frac{ek_n^2 z_0}{2\pi\omega\epsilon R_0} \sin\theta \left(\int \frac{1 - z'\epsilon_0 \cos\theta}{R^3} G_1\,\mathrm{d}z' + \frac{2}{k_n R_0} \int \frac{G}{R^2}\,\mathrm{d}z' \right)
\end{aligned} \tag{4.11}$$

where

$$F = \cos\psi - \frac{1}{k_n R_0 R}\sin\psi \qquad G = \sin\psi + \frac{1}{k_n R_0 R}\cos\psi$$

$$F_1 = \sin\psi + 3\frac{\cos\psi}{k_n R_0 R} - 3\frac{\sin\psi}{k_n^2 R_0^2 R^2} \qquad G_1 = \cos\psi - 3\frac{\sin\psi}{k_n R_0 R} - 3\frac{\cos\psi}{k_n^2 R_0^2 R^2}$$

$$\psi = k_n R_0 \left(\frac{z'\epsilon_0}{\beta_n} + R \right) \qquad R = (1 - 2z'\epsilon_0 \cos\theta + \epsilon_0^2 z'^2)^{1/2} \qquad \epsilon_0 = z_0/R_0.$$

The z' integration in (4.10) is performed over the interval $(-1, 1)$. For $\epsilon_0 \ll 1$ and $k_n R_0 \gg 1$, $S(\omega)$ given by (4.10) transforms into Tamm's formula (2.8):

$$S_T = \frac{e^2 \sin^2\theta}{\pi^2 nc} \left[\frac{\sin k_n z_0(\cos\theta - 1/\beta_n)}{\cos\theta - 1/\beta_n} \right]^2. \tag{4.12}$$

There are three geometric parameters of the length dimension entering into (4.11) and (4.12): the motion interval $L = 2z_0$; the radius of the observation sphere R_0 and the vacuum wavelength $\lambda = 2\pi c/\omega$ related to the medium wavelength $\lambda_n = \lambda/n$. It is essential that these parameters enter into the energy flux and field strengths through dimensionless combinations,

$$\epsilon_0 = \frac{z_0}{R_0} = \frac{L}{2R_0} \qquad k_n z_0 = \frac{\pi n L}{\lambda} \qquad k_n R_0 = \frac{2\pi n R_0}{\lambda} = \frac{k_n z_0}{\epsilon_0}.$$

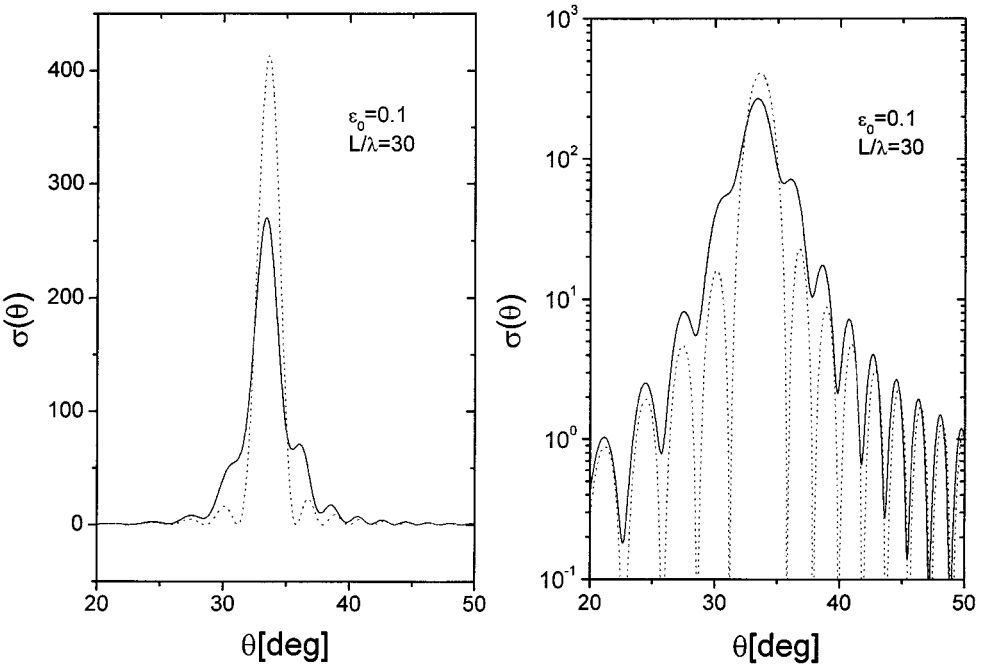

Figure 5. Exact (full curve) and Tamm's approximate (dotted curve) angular dependences for $\epsilon_0 = z_0/R_0 = 0.1$, $L/\lambda = 30$, $\beta_n = 1.2$, $n = 1.5$ in the linear (left) and logarithmic (right) scales. In figures 5–8, z_0 and R_0 are the same but λ changes.

Thus, if only λ changes, ϵ_0 remains the same, but $k_n z_0$ and $k_n R_0$ vary. The typical exact (4.10) and Tamm's (4.12) intensities for the fixed $\epsilon_0 = 0.1$ and different L/λ are shown in figures 5–8 in logarithmic and usual scales. For convenience, we made the intensities dimensionless (dividing them by the factor e^2/c). All the subsequent figures refer to $n = 1.5$, $\beta_n = 1.2$. We see that Tamm's intensities are close to the exact ones for small and moderate L/λ ratios (figure 5). Their difference becomes essential for large L/λ (figures 6–8). These figures demonstrate that the disagreement between Tamm's and the exact intensities may be essential despite the fact that ϵ_0 is small ($\epsilon_0 = 0.1$), and $k_n R_0$ is large ($k_n R_0 \approx 5 \times 10^3$, 10^4 and 2×10^4 for figures 6–8, respectively). The reason for this is due to the violation of (4.5). In fact, the left-hand side of (4.5) equals approximately 20, 40 and 100 for the situations shown in figures 6–8, respectively.

Another degree of freedom is to change only R_0. In this case, L/λ remains the same, but ϵ_0 and $k_n R_0$ change. The typical intensities for $L/\lambda = 200$ and different ϵ_0 are shown in figures 7, 9 and 10. It is seen that disagreement between Tamm's intensity and the exact one increases sharply when z_0 approaches R_0 (as it should).

The last possibility is to change only z_0. In the language of dimensionless variables, this means that $k_n R_0$ remains the same, while $k_n z_0$ and ϵ_0 change in such a way that their ratio remains the same. Figures 7, 11 and 12 demonstrate that the disagreement between Tamm's and the exact intensities increases with z_0.

Previously, the experimentally observed broadening of the Cherenkov angular spectrum was attributed to the energy loss of a charged particle during its motion in the medium [18, 19]. However, figures 6–8, and 10–12 demonstrate that the above broadening may be well associated with the violation of conditions (4.1)–(4.7). To be more specific, we turn to [19] in which the

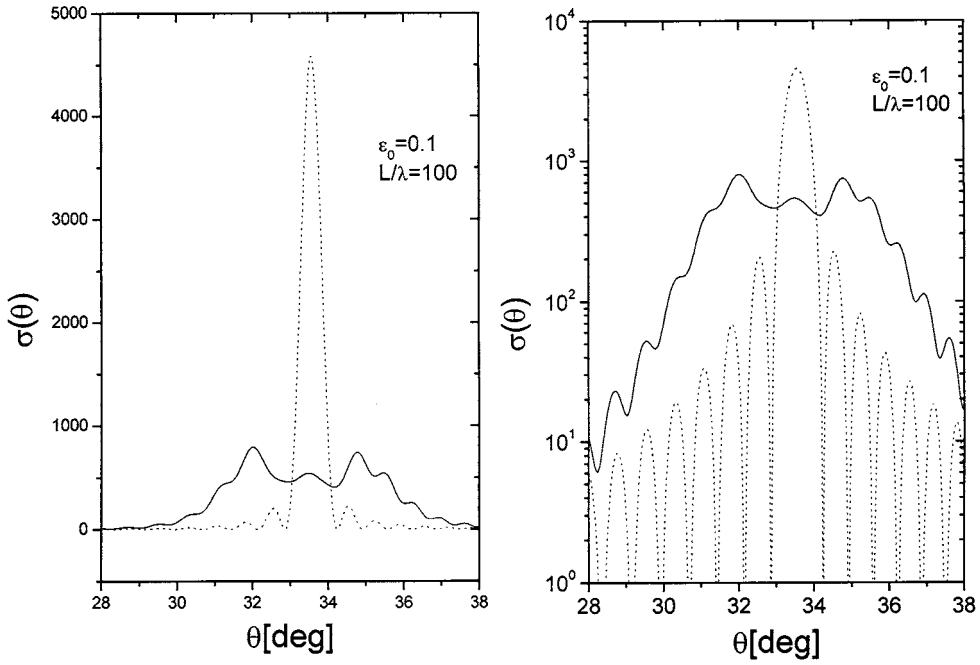

Figure 6. The same as in figure 5, but for smaller λ corresponding to $L/\lambda = 100$. The deviation of the approximate curve from the exact one increases as λ diminishes.

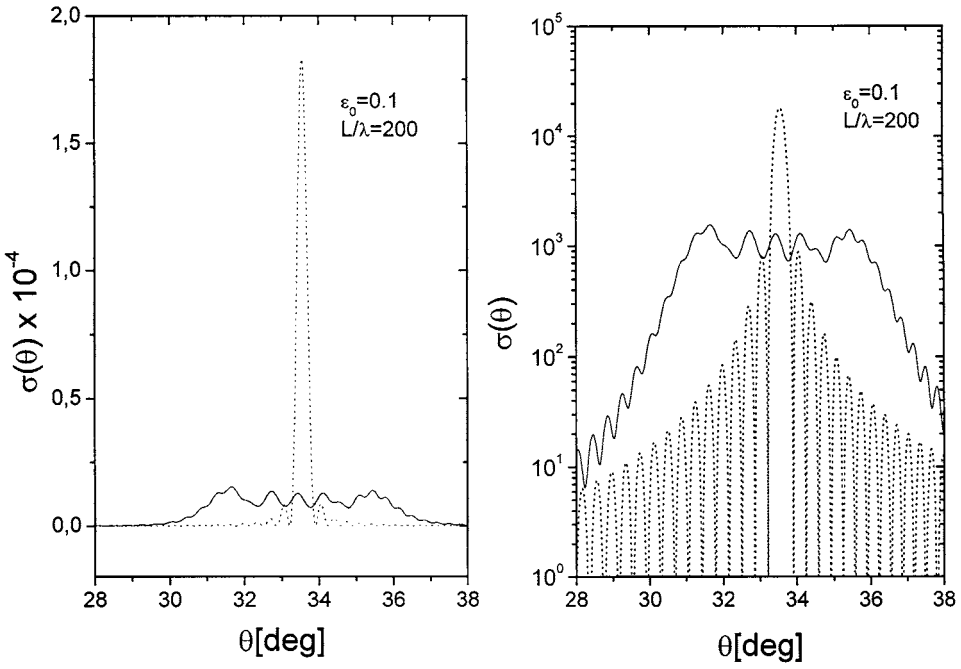

Figure 7. The same as in figure 6, but for $L/\lambda = 200$.

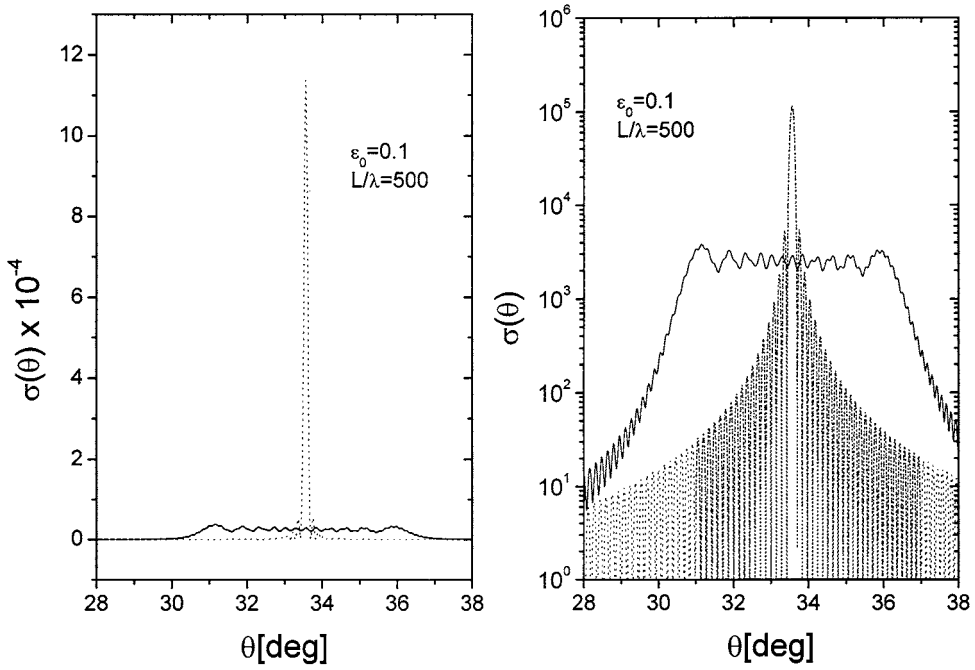

Figure 8. The same as in figure 6, but for $L/\lambda = 500$.

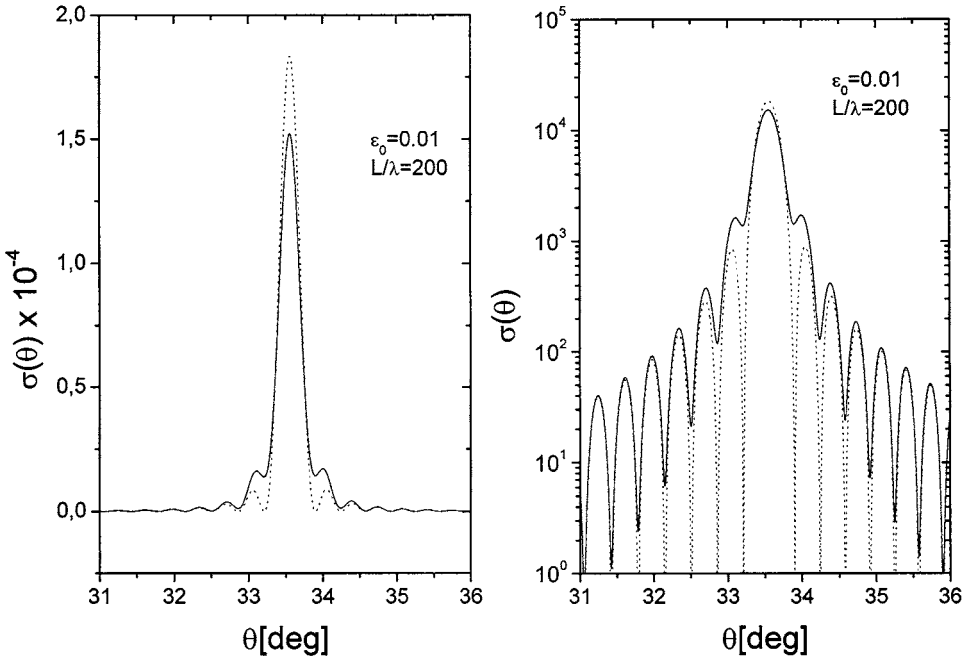

Figure 9. For small ϵ_0, the deviation of the approximate curve from the exact one is not very large. In figures 7, 9 and 10, L and λ are the same, but R_0 changes.

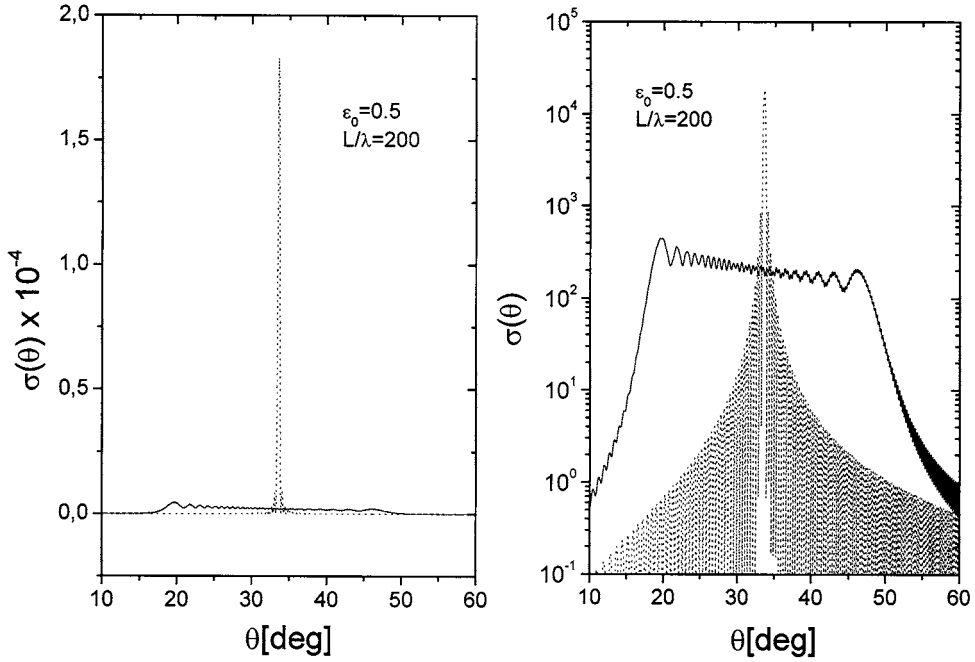

Figure 10. The same as in figure 9, but for greater R_0 corresponding to $\epsilon_0 = 0.5$. The deviation of the approximate curve from the exact one is essential.

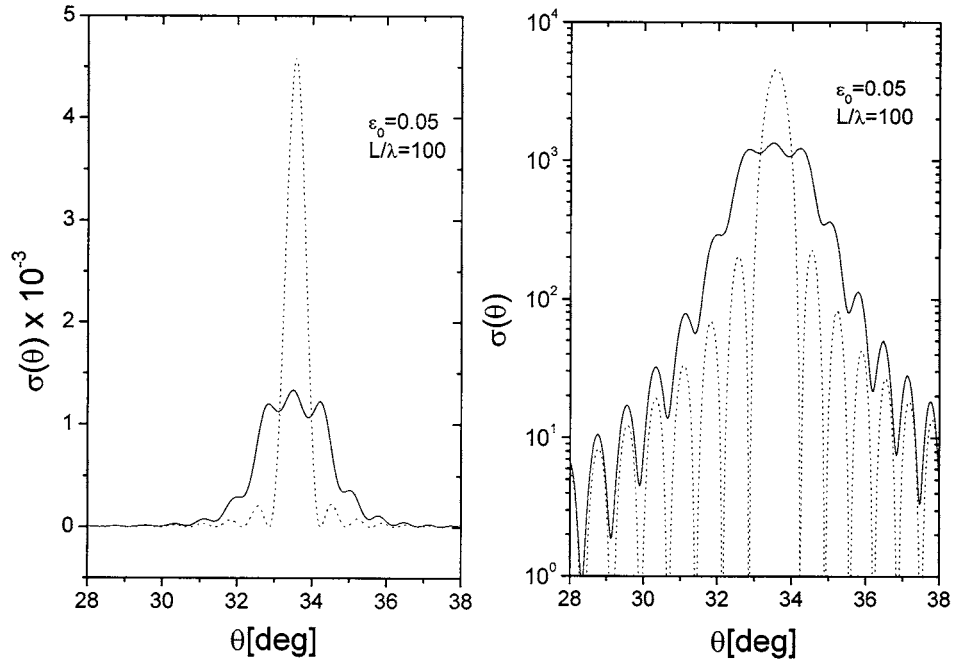

Figure 11. For small and moderate z_0 corresponding to $\epsilon = 0.05$, the deviation of the approximate curve from the exact one is not essential. Figures 7, 11 and 12 correspond to the same λ and R_0, but different z_0.

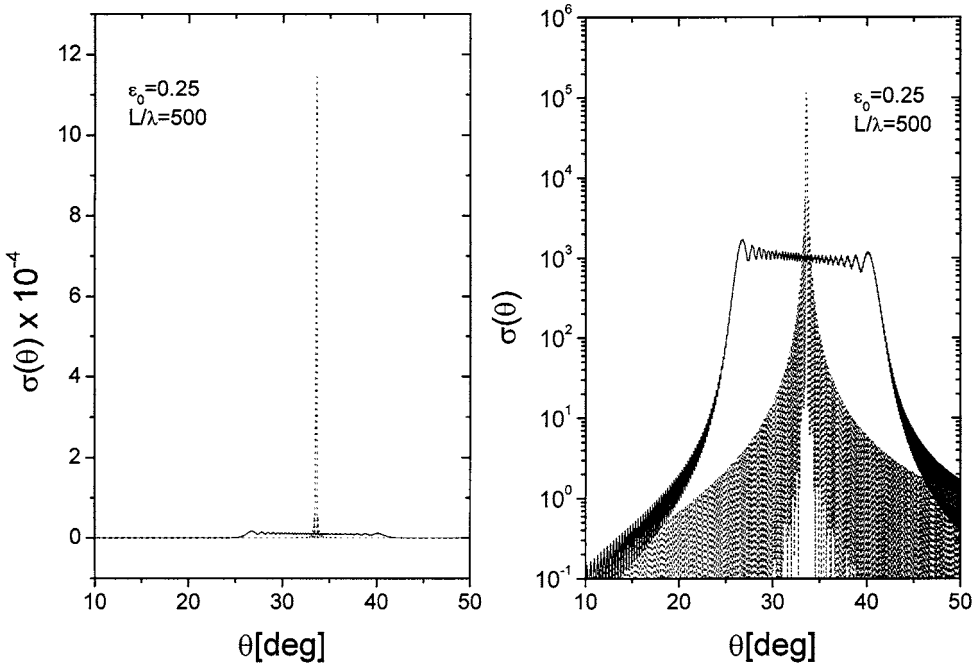

Figure 12. The same as in figure 11 but for larger z_0 corresponding to $\epsilon = 0.25$. The deviation of the approximate curve from the exact one becomes essential when z_0 approaches R_0.

angular distribution of the radiation ($\lambda \approx 4 \times 10^{-5}$ cm) arising from the passage of Au heavy ions ($\beta \approx 0.87$) through the LiF slab ($n \approx 1.39$) of width 0.5 cm was studied. Substituting these parameters into (4.5), we see that the left-hand side of this equation coincides with π for the observation sphere radius $R_0 \approx 400$ m. Obviously, this value is unrealistic. Since the realistic R_0 is about 1–2 m, a strong violation of (4.5) takes place.

The moral of this section is that one should be very careful when applying Tamm's formula (2.8) to the analysis of experimental data. The validity of conditions (4.1)–(4.7) ensuring the validity of (2.8) should be verified. The exact energy flux (4.10) should be used if these conditions are violated.

5. Conclusion

Let us briefly summarize the main results obtained.

(a) Within the framework of Schwinger's approach, closed expressions are obtained for the frequency and angular distributions for the energy radiated by a point charge moving uniformly in a medium in a finite space interval (Tamm's problem). They generalize the formulae given by Frank and Tamm and are reduced to them in particular cases.

(b) Tamm's approximate formula describing the frequency-angular distribution of the radiated energy in Tamm's problem is compared with the exact one. Criteria for the validity of Tamm's formula are checked by numerical calculations.

Acknowledgment

The authors are indebted to Professor V P Zrelov for many stimulating and interesting discussions.

References

[1] Tamm I E 1939 *J. Phys. USSR* **1** 439
[2] Lawson J D 1954 *Phil. Mag.* **45** 748
[3] Lawson J D 1965 *Am. Phys. J.* **33** 1002
[4] Zrelov V P and Ruzicka J 1989 *Chech. J. Phys.* B 368–83
[5] Zrelov V P and Ruzicka J 1992 *Chech. J. Phys.* **42** 45–57
[6] Afanasiev G N, Beshtoev Kh and Stepanovsky 1996 *Helv. Phys. Acta* **69** 111–29
[7] Afanasiev G N, Kartavenko V G and Stepanovsky Yu P 1999 *J. Phys.* D **32** 2029
[8] Schwinger J 1949 *Phys. Rev.* A **75** 1912
[9] Schwinger J and Tsai W Y 1976 *Ann. Phys., NY* **96** 303
[10] Erber T, White D, Tsai W Y and Latal H G 1976 *Ann. Phys., NY* **102** 405
[11] Frank I M 1988 *Vavilov–Cherenkov Radiation* (Moscow: Nauka) in Russian
[12] Zrelov V P 1970 *Vaviliov–Cherenkov Radiation in High Energy Physics (Israel Program for Scientific Translations 1970)*
[13] Aitken D K *et al* 1963 *Proc. Phys. Soc.* **83** 710
[14] Zrelov V P *et al* 1983 *Nucl. Instrum. Methods* **215** 141
Zrelov V P *et al* 1988 *Nucl. Instrum. Methods* A **270** 62
[15] Fano R M, Chu L J and Adler R B 1960 *Electromagnetic Fields, Energy and Forces* (New York: Wiley)
[16] Kobzev A P and Frank I M 1981 *Yad. Fiz.* **34** 125
[17] Kobzev A P, Krawczyk A and Rutkowski J 1988 *Acta Phys. Pol.* B **119** 853
[18] Kuzmin E S and Tarasov A V 1993 *Rapid Commun. JINR* 4/61/-93 p 64
[19] Krupa L, Ruzicka J and Zrelov V P 1995 *JINR Preprint* P2-95-381